Loss of Inner Retinal Neurons After Retinal Ischemia in Rats

Heiko Schmid, Marina Renner, H. Burkhard Dick, and Stephanie C. Joachim

Experimental Eye Research Institute, Ruhr University Eye Hospital, Bochum, Germany

Correspondence: Stephanie C. Joachim, Head of Experimental Eye Research Institute, Ruhr University Eye Hospital, In der Schornau 23-25, 44892 Bochum, Germany; stephanie.joachim@rub.de.

Submitted: October 1, 2013
Accepted: March 24, 2014

Citation: Schmid H, Renner M, Dick HB, Joachim SC. Loss of inner retinal neurons after retinal ischemia in rats. *Invest Ophthalmol Vis Sci*. 2014;55:2777–2787. DOI:10.1167/iovs.13-13372

Purpose. Ischemia is a risk factor for eye diseases like ocular vein occlusion or glaucoma. To investigate effects of ischemia-reperfusion (I/R) a lot of different animal models are used, studying one or two different cell types, which creates heterogeneity of data. The aim of this study was to investigate the function and morphology of the whole retina and different retinal cell types in an I/R model.

Methods. I/R was induced by elevating the intraocular pressure in the right eyes of rats. Twenty-one days after ischemia, electroretinogram measurements were performed. Changes in layer thickness were investigated. Changes of RGC, amacrine-, rod bipolar-, and glia cells as well as presence of apoptosis were analyzed immunohistologically.

Results. A-wave- and b-wave amplitudes were decreased; histology showed a reduction of RGC- and inner plexiform layer thickness and a 29% loss of RGCs occurred in ischemic eyes ($P = 0.016$). An increase of apoptotic cells was detected in the GCL and INL of ischemic retinas ($P < 0.05$). Also, a loss of cholinergic amacrine cells (control: 11 ± 1 cells/mm, I/R: 4 ± 1 cells/mm, $P < 0.001$), but no change in rod bipolar cell numbers was noted.

Conclusions. Our study allowed a comparison of the effects of I/R for different retinal cell types. Cells in the outer retina seemed to be more resistant to ischemic damage compared with cells of the inner retina. We hypothesize that a degenerative process, like a secondary wave of apoptosis, occurs 21 days after I/R, causing progressive damage in the retina.

Keywords: ischemia-reperfusion, apoptosis, electroretinogram, amacrine cells, bipolar cells

Blood deficiency or a complete lack of blood supply of the eye, often referred to "retinal ischemia" is a common cause of various retinal diseases and visual impairments, which can lead to blindness.[1] Diseases associated with ischemia include central retinal artery occlusion, ischemic central vein occlusion, ocular ischemic syndrome, hypertension, diabetic retinopathy, and glaucoma.[1–7] Due to a drop of oxygen and nutrients caused by a reduction of blood supply in various retinal layers, ischemia occurs. Cascades of events leading to mitochondrial, oxidative, stress-mediated cell death are caused by reperfusion with blood.[1,7,8]

In recent years, research has been performed to investigate the effects of ischemic injuries in the retina.[9–11] However, although retinal ischemia is a global disease affecting the whole retina, most studies focused on a few or a single retinal cell type. Specifically the degenerative changes, like the retinal ganglion cell (RGC) loss or alterations in RGC axons, are well documented. This has created a heterogeneity of data originating from different ischemia models using different strains or species. Although it is known that ischemic injuries are long lasting, the effects and mechanisms of ischemic insults in the retina at a later point in time have not been studied intensively yet. Lately, morphological and functional studies in other animal models of elevated intraocular pressure (IOP) revealed that neuronal populations in the inner- and outer nuclear layers of the retina might also be affected by ischemic injuries.[12–17]

In this study, we investigated the effect of transient ischemia in the retina 21 days after I/R, common model to investigate degenerative diseases of the retina.[18] We used a combination of ERG measurements and immunohistology to analyze the effects of ischemia on the different retinal cell types including RGCs, amacrine cells, bipolar cells, and glia cells. Additionally, we investigated apoptotic processes and the activation of phagocytes in the ischemic retina. Ischemia led to electrophysiological and histological changes of the inner retina, especially of the amacrine, bipolar, and Müller cells. ERG recordings indicated a disruption of synaptic connectivity in the outer retina, although no loss of rod bipolar cells occurred. Apoptotic processes were accompanied by an increase of phagocytes, likely due to a second wave of degeneration. Taken together, we conclude, that amacrine cells and their dendrites as well as RGC are most affected by I/R.

Materials and Methods

Animals

Male brown Norway rats (6 weeks old; Charles River Laboratories, Sulzfeld, Germany) were housed and maintained under environmentally controlled conditions in a 12-hour light/dark cycle with access to food and water ad libitum in the absence of pathogens. All experiments that involved animal use were performed in compliance with the ARVO Statement for the Use of Animals in Ophthalmic and Vision Research. These experiments have been approved by the local animal care committee.

Induction of Ischemia-Reperfusion

Rats ($n = 5$) were anesthetized with a ketamine/xylazine/vetranquil cocktail (0.65/0.65/0.2 mL). Right eyes were dilated with 5% tropicamide (Pharma Stulln GmbH, Stulln, Germany) followed by topical anesthesia with conjuncain EDO (Bausch & Lomb GmbH, Berlin, Germany). Additionally, caprofen (0.2 mL/100 g; Pfizer Deutschland GmbH, Berlin, Germany) was injected subcutaneously to avoid inflammation. A 27-gauge needle (Terumo Europe, Leuven, Belgium) connected to a saline reservoir containing 0.9% NaCl (Fresenius SE & Co. KGaA, Bad Homburg, Germany) was placed in the anterior chamber of the right eye. Intraocular pressure (IOP) was raised to 140 mm Hg for 60 minutes by elevating the saline reservoir. Retinal ischemia was confirmed by observing whitening of the retina and reperfusion was reassured by observing the returning blood flow with an ophthalmoscope (Mini 300; Heine Optotechnik, Herrsching, Germany). Left eyes were left untreated and served as controls. During the whole surgery and for anesthesia recovering, the animals were kept on a heating pad.

Intraocular Pressure Measurements

Before and after I/R, IOP was measured in both eyes of each rat with a tonometer (TonoLab; Icare, Oy, Finland) as previously described.[19,20] Ten measurements of each eye were obtained 4 days before as well as 1, 7, 14, and 21 days after induction of I/R. Means of each point in time were calculated for both groups and used for analysis.

Electroretinogram Measurement

Before performing the ERG under dim red light, rats were dark-adapted overnight. The function of the retina was monitored using full-field flash electroretinography (HMsERG system; OcuScience LLC, Rolla, MO, USA) 21 days after I/R.[21] After being anesthetized with a ketamine/xylazine cocktail (100/4 mg/kg), eyes were dilated with tropicamide 5% and topically anesthetized with conjuncain. Body temperature was maintained at 37°C with a feedback temperature controller (TC-1000; CWE Inc., Ardmore, PA, USA). Reference electrodes were placed subcutaneously below the right and left ear and a ground electrode was placed in the base of the tail. Silver thread recording electrodes were placed in the center of the cornea after application of methocel (Omni Vision, Puchheim, Germany). Clear zero power contact lenses were placed on the cornea to prevent the electrodes from moving or detaching. Before measurement, the electroretinography equipment (OcuScience LLC) was covered with a faraday cage. Scotopic flash ERGs were recorded at 0.1, 0.3, 1, 3, 10, and 25 cd/m^2. Signals obtained from the corneal surface were amplified, digitized, averaged, and stored using commercial software (ERGView 4.380R; OcuScience LLC) for later analysis. A 50 Hz-filtering of the data was applied before evaluating amplitude and latency of the a- and b-wave. Data was then transferred to a spreadsheet program (Excel; Microsoft Corp., Redmond, WA, USA) for statistical analysis.

Histology of Retinal Cross-Sections

Twenty-one days after I/R rats were killed and the eyes enucleated ($n = 5$ eyes/group). The eyes were fixed in 4% paraformaldehyde and embedded OCT (Tissue-Tek; Thermo Fisher Scientific, Cheshire, UK). Retinal cross-sections 10-μm thick were cut on a microtome (Thermo Fisher Scientific, Walldorf, Germany).

Hematoxylin & eosin stain (H&E) was used to investigate structural changes as well as changes in the thickness of the retinal layers. Therefore, after de- and rehydration in 70% to 100% ethanol, retina cross-sections were stained with H&E.[22,23] Subsequently, all slides were again dehydrated in ethanol followed by incubation in xylene before being mounted with quick-hardening medium (Eukitt; O-Kindler GmbH & Co., Freiburg, Germany). Three H&E stained retina sections of each eye were photographed at a distance of 1500 μm dorsal and ventral to the optic nerve with a microscope equipped with a charge-coupled device (CCD) camera (Axio Imager M1; Carl Zeiss Microscopy, Oberkochen, Germany). Images were analyzed with the measuring tool of image analysis software (ZEN 2011, v. 1.0.1.0.; Carl Zeiss Microscopy). Measurement of the thickness of the whole retina (excluding the outer segments); GCL; inner plexiform layer (IPL); inner nuclear layer (INL); outer plexiform layer (OPL); and outer nuclear layer (ONL) was performed. For each layer, three measurements per photo were averaged. Data was then transferred to a statistics and analytics software package (Statistica, v. 10.0; StatSoft, Tulsa, OK, USA) for further analysis.

Immunohistochemistry of Retinal Cross-Sections

Retinal cross-sections (10-μm thick, $n = 5$ eyes/group) were used for immunohistochemistry. The sections were dried and rehydrated in PBS and then blocked in 10% appropriate serum in 0.1% Triton X in PBS. Six retinal sections per animals were used for each staining. In general, the same camera setting, including exposure time, was applied on all images for each staining protocol. Per section four pictures were obtained using a fluorescence microscope (Carl Zeiss Microscopy) equipped with a CCD camera (Axiocam HRc; Carl Zeiss Microscopy). The digitalized images were transferred to photo editing software (Corel PaintShop Photo Pro, v. 13; Corel Corp., Fremont, CA, USA) and excerpts were cut out.

RGC were stained with anti-Brn-3a, a specific RGC marker.[24,25] Anti-TRADD, anti–TNF-R1, anti-cleaved caspase 3 (cl-caspase 3), and anti-FasL was used to label the activation of apoptosis. Activated microglia cells and macrophages were labeled with anti-ED1.[26] Rod bipolar cells were stained with anti-PKCα and cholinergic amacrine cells were marked with anticholine acetyltransferase (ChAT). The macroglial cells were investigated with anti-glial fibrillary acidic protein (GFAP) and anti-vimentin. Appropriate secondary antibodies were used to label the different cell types. Detailed information of the applied primary and secondary antibodies is listed in the Table. DAPI was used as a nuclear stain. All slides were mounted with antifade medium (Fluoro-Mount; Dianova, Hamburg, Germany).

Brn3a$^+$, ChAT$^+$, and PKCα$^+$ cells were counted in four photos per retinal cross-section. The distance to the optic nerve was 300 and 3100 μm, respectively. Colocalization of cl-caspase 3 and Brn-3a was counted in six photos per retinal cross-sections at a distance of 300, 1500, and 3100 μm dorsal and ventral to the optic nerve. All images were analyzed under masked conditions using ImageJ software version 1.44p (http://imagej.nih.gov/ij/; provided in the public domain by the National Institutes of Health [NIH], Bethesda, MD, USA). For the GFAP and vimentin staining analysis the pictures were transferred in ImageJ (NIH).[27] First, the images were transformed into gray scale. After background subtraction (GFAP and vimentin: 50 pixels), the upper and lower threshold was set (GFAP: lower threshold: 3.252, upper threshold: 80; vimentin: 3.005, upper threshold: 80). Background subtraction and upper and lower threshold represent mean values of the manually analyzed images of both control and ischemia eyes.

Investigative Ophthalmology & Visual Science

TABLE. List of Primary and Adequate Secondary Antibodies Used to Label RGCs, Apoptotic Cells, Cholinergic Amacrine Cells, Rod Bipolar Cells, and Glia Cells

Primary Antibody	Dilution	Source	Secondary Antibody	Dilution	Source
Anti-Brn-3a	1:100	Santa Cruz Biotechnology, Heidelberg, Germany	Donkey anti-goat Alexa488	1:500	Dianova, Hamburg, Germany
Anti-ChAT	1:250	Millipore Corp., Billerica, MA, USA	Donkey anti-rabbit Alexa555	1:500	Invitrogen, Darmstadt, Germany
Anti-PKCα	1:500	Santa Cruz Biotechnology	Goat anti-mouse Alexa488	1:500	Life Technologies, Darmstadt, Germany
Anti-GFAP	1:400	Millipore Corp., Darmstadt, Germany	Donkey anti-chicken Cy3	1:500	Millipore Corp., Billerica, MA, USA
Anti-vimentin	1:500	Sigma-Aldrich, Munich, Germany	Goat anti-mouse Alexa488	1:500	Life Technologies
Anti-cleaved caspase 3	1:400	Biozol, Echingen, Germany	Donkey anti-rabbit Alexa555	1:500	Invitrogen
Anti TRADD	1:100	Abcam, Cambridge, UK	Goat anti-rabbit Alexa488	1:500	Invitrogen
Anti-TNF-R1	1:100	Santa Cruz Biotechnology	Goat anti-mouse Alexa555	1:700	Invitrogen
Anti-FasL	1:100	Abcam	Donkey anti-rabbit Alexa555	1:600	Invitrogen
Anti-ED1	1:250	Millipore Corp., Billerica, MA, USA	Goat anti-mouse Alexa488	1:500	Life Technologies

The percentage of GFAP$^+$ and vimentin$^+$ labeled area was measured in each picture using an ImageJ macro (NIH).

Statistics

Data are presented as mean ± SEM unless otherwise noted. ERG and histology data of the two groups were compared using two-tailed Student's *t*-test (StatSoft). *P* values below 0.05 were considered statistically significant.

RESULTS

No Changes in Intraocular Pressure

To observe possible alterations in the intraocular IOP during the study it was measured before and 1, 7, 14, and 21 days after I/R. At each point in time, no difference in the mean IOP could be observed between the ischemic and control eyes (Figs. 1A, 1B). Four days before I/R, a mean IOP of 9.7 ± 0.1 mm Hg was measured in the control eyes and of 9.6 ± 0.1 mm Hg in the ischemic eyes ($P = 0.5$, Fig. 1A). The IOP stayed within this range up to 3 weeks after I/R (ischemia: 9.5 ± 0.1 mm Hg; control: 9.7 ± 0.1 mm Hg, $P = 0.4$; Fig. 1A).

Loss of Retinal Functionality After Ischemia-Reperfusion

Twenty-one days after, I/R scotopic ERG was recorded and the amplitudes and latencies of the a- and b-wave were analyzed (Fig. 2). The reduction of a- and b-wave amplitude is visible in a representative ERG-trace at 3 cd/m^2 of an ischemic eye and its contralateral control eye 21 days after I/R (Fig. 2A). Between 0.1 and 25 cd/m^2, the amplitudes of the a-wave of the control and ischemic eyes increased steadily (Fig. 2B). However, the amplitudes of the a-wave of ischemic eyes were significantly reduced at light intensities of 0.1 to 10 cd/m^2 compared with control ($P < 0.05$, Fig. 2B). The amplitudes of the b-wave of control and ischemic eyes also increased steadily between the flash intensities of 0.1 to 25 cd/m^2, but were significantly reduced in the ischemic eyes at all flash intensities ($P < 0.001$, Fig. 2C). The implicit times of the a-wave of both control and ischemic eyes got continuously reduced using light intensities between 0.1 and 25 cd/m^2, but no statistical difference of the implicit times of the a-wave between both groups was observed at any light intensity ($P > 0.05$; Fig. 2D). For the implicit time of the b-wave, a significant decrease could only be observed at a flash intensity of 0.1 cd/m^2 (control: 64.6 ± 0.8 ms, ischemia: 52.0 ± 3.6 ms, $P = 0.009$; Fig. 2E).

A

Duration	Control	Ischemia	p-value
-4	9.7±0.1	9.6±0.1	0.5
1	9.9±0.1	9.8±0.1	0.8
7	9.7±0.1	9.5±0.1	0.1
14	9.8±0.1	9.6±0.1	0.2
21	9.7±0.1	9.5±0.1	0.4

B

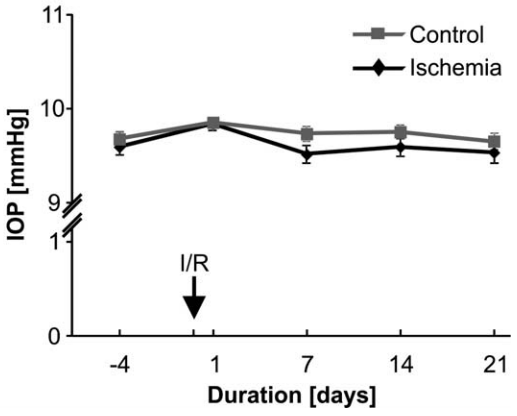

FIGURE 1. (**A**) Statistical analysis of the IOP measurements. The mean values and standard deviation of the ischemic and control group are given. Student's *t*-test was used to acquire *P* values. (**B**) Measurement of the IOP before and 1, 7, 14, and 21 days after I/R. IOP stayed within the same level at all time points. At day 0 (*arrow*), I/R was initiated. Data are presented as mean ± SD.

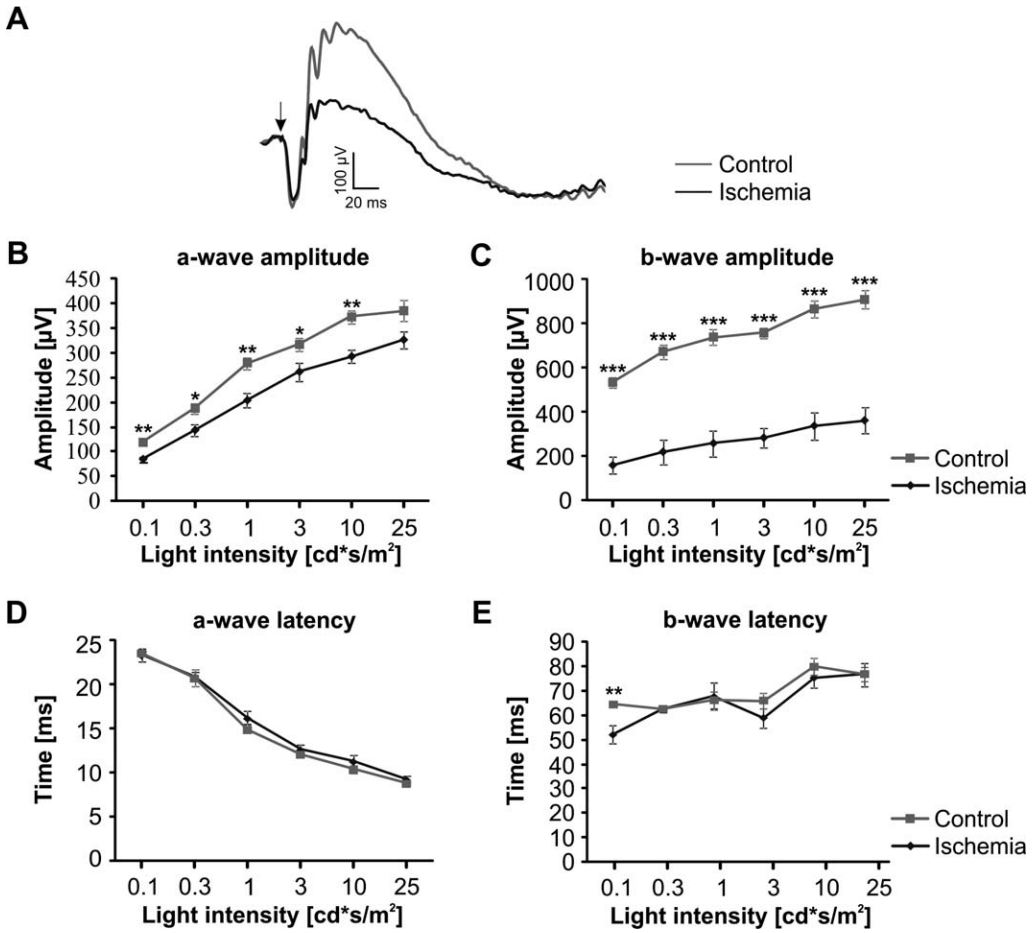

Figure 2. (**A**) Representative ERG recording at 3 cd/m^2 of a control eye (*gray*) and a contralateral ischemic eye (*black*). The *arrow* represents the start of the light stimulus. A reduction of the a- and b-wave can be noted in the ischemic eye. (**B**) Changes in the amplitude of the a-wave of ischemic eyes at light intensities ranging from 0.1 to 25 cd/m^2. For 0.1 to 10 cd/m^2, the amplitude of the a-wave was significantly reduced in the ischemic eyes compared to control. (**C**) Changes of the b-wave amplitude of control and ischemic eyes at 0.1 to 25 cd/m^2 light intensities. The amplitude of the b-wave was significantly reduced in the ischemic eye at all intensities. (**D**) Changes in the a-wave latencies of control and ischemic eyes. No differences between the two groups were observed. (**E**) Response latency in the b-wave in control and ischemic eyes. At 0.1 cd/m^2 a significant reduction of the b-wave latency was noted. All data are presented as means ± SEM. $^*P < 0.05$. $^{**}P < 0.01$. $^{***}P < 0.001$.

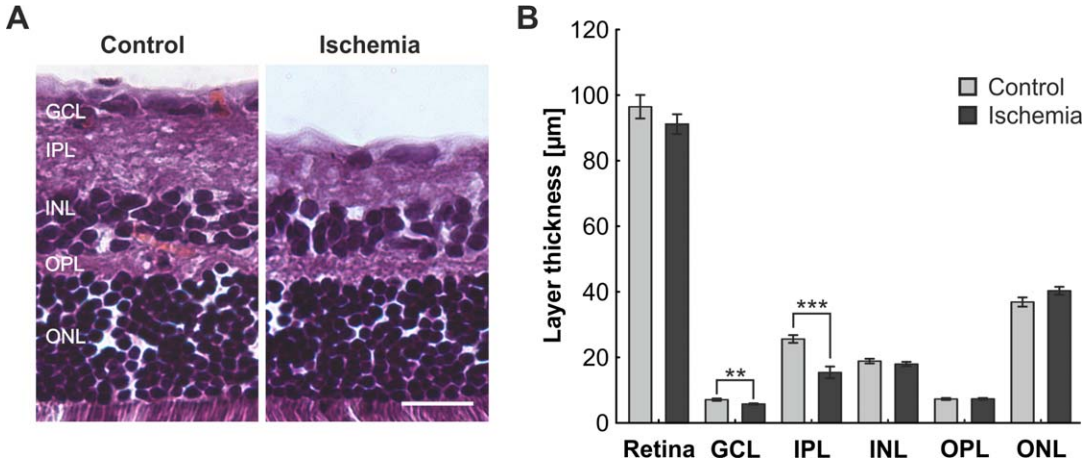

Figure 3. (**A**) Control and ischemic retinas stained with H&E 21 days after I/R. A reduction of IPL thickness and loss of cells in the GCL was visible. (**B**) The thickness of the GCL and IPL of the ischemic eyes was significantly reduced compared with controls (GCL: $P = 0.0022$; IPL: $P < 0.001$). No differences were observed in the INL, OPL, ONL, and the overall thickness of the retina. Data are presented as mean ± SEM. $^{**}P < 0.01$. $^{***}P < 0.001$. *Scale bar*: 20 µm.

Investigative Ophthalmology & Visual Science

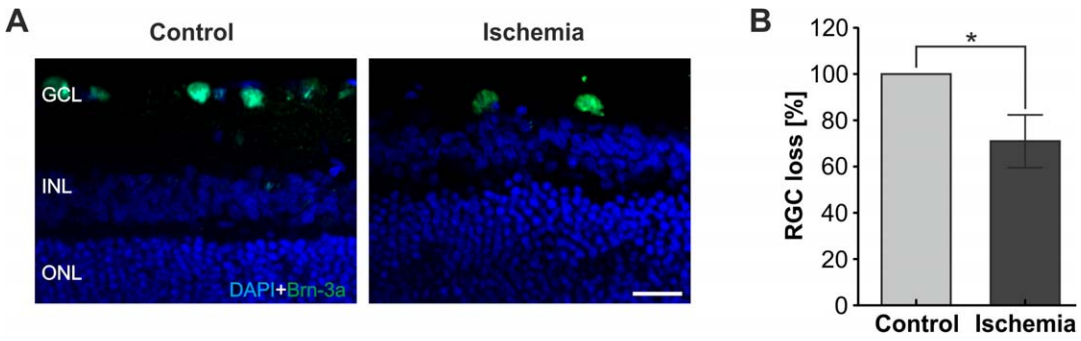

Figure 4. (**A**) Brn-3a stained RGCs (*green*) and cell nuclei (DAPI, *blue*) of the control and ischemic eye at 21 days. Less Brn-3a$^+$ RGC were observed in ischemic retinas. (**B**) RGC numbers were significantly reduced by 29.4% in the ischemic eyes compared with control ($P = 0.0332$). Data are presented as mean ± SEM. $^*P < 0.05$. *Scale bar*: 20 μm.

Changes in the Retinal Morphology

H&E stained retinas were used for evaluation of retinal layers. The integrity of the retina stayed intact after I/R, but a decrease in the thickness of the GCL and IPL was noted (Fig. 3A). The quantification displayed a significant reduction of the GCL (control: 7.1 ± 0.4 μm; ischemia: 5.8 ± 0.2 μm; $P = 0.0022$) and the IPL (control: 25.6 ± 1.2 μm; ischemia: 15.4 ± 1.8 μm; $P < 0.001$; Fig. 3B). However, no difference in the thickness of the whole retina, the INL, OPL, and ONL was noted (Fig. 3B).

Retinal Ganglion Cell Loss After Ischemia-Reperfusion

In order to analyze RGC number, cross sections of ischemic and control retinas were stained with anti-Brn-3a. Fewer RGCs were noted in ischemic retinas (Fig. 4A). Quantification of RGC in control and ischemic retinas resulted in a 29.4% loss of RGC in the ischemic eyes ($P = 0.0332$; Fig. 4B).

Activation of Phagocytes in Ischemic Retinas

Apoptosis triggers the activation and proliferation of microglia and macrophages.[28] Therefore, activated microglia and macrophages were detected. ED1$^+$ cells were noted in the GCL, IPL, and INL of retinas of both groups (Fig. 5A), while the OPL and INL showed no positive staining for ED1. Statistical analysis revealed significant higher numbers of ED1$^+$ microglia and macrophages in the GCL, IPL, and INL of ischemic eyes (8 ± 0.3 cells/mm) compared with controls (2 ± 0.3 cells/mm, $P <$ 0.001; Fig. 5B).

Increased Apoptosis Rate in the Inner Retina of Ischemic Eyes

Anti-cleaved caspase 3 (cl-caspase 3) was used in combination with anti-Brn-3a to detect apoptotic RGCs. Only few cl-caspase 3 signals were present in the RGC of both groups after 21 days (Fig. 6A). A significant increase of cl-caspase 3$^+$ retinal ganglion cells was detected in ischemic eyes (3% ± 0.9%) compared with control eyes (1% ± 0.3%, $P = 0.0164$; Fig. 6B). To further investigate apoptosis at 21 days, a staining against the TNF-R1 and TNF-R1 associated death protein (TRADD) was performed. In control and ischemic retinas, anti-TRADD and anti-TNF-R1 staining was limited to the GCL (Fig. 6C). We further observed TNF-R1 being localized in the center of the cell while TRADD seemed to be present in the soma of the cell (Fig. 6A). Counting of the colocalized TNF-R1$^+$ and TRADD$^+$ staining revealed a loss of the association between TNF-R1 and TRADD in ischemic retinas (10 ± 0.8 cells/mm) compared with controls (14 ± 1.1 cells/mm, $P = 0.0012$, Fig. 6D). Additionally, we stained for FasL. The nuclei of FasL$^+$ cells were encircled by FasL and could be detected in both groups, predominantly in the INL (Fig. 6E). A significant increase of FasL$^+$ cells in the ischemic retinas (16 ± 0.8 cells/mm) was observed compared with control retinas (10 ± 0.7 cells/mm, $P < 0.001$; Fig. 6F).

Cholinergic Amacrine Cell Loss After Ischemia-Reperfusion

Cholinergic amacrine cells were labeled witch anti-ChAT.[28,29] In the control rat retinas, the cell bodies of cholinergic amacrine cells in the INL and GCL as well as two distinct bands

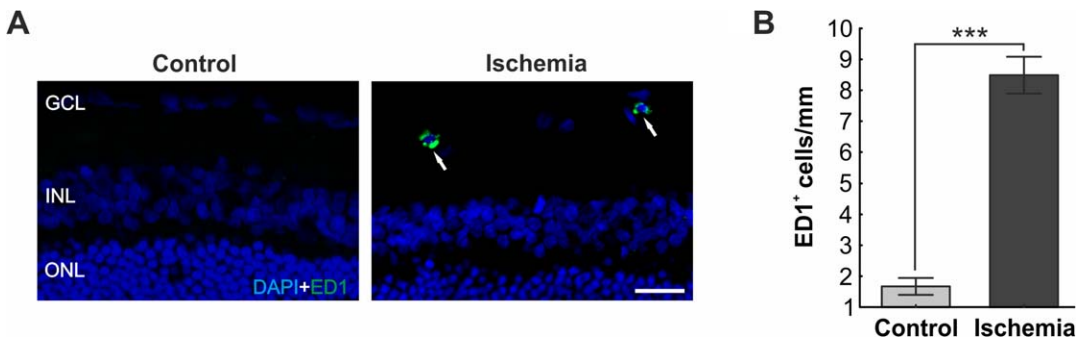

Figure 5. (**A**) ED1-stained activated microglia and macrophages. ED1$^+$ cells (*green*, *arrows*) were only present in the GCL, IPL, and INL. (**B**) Counting of ED1$^+$ cells revealed a significant increase of activated microglia and macrophages in ischemic eyes (8 ± 0.6 cells/mm) compared with control (2 ± 0.3 cells/mm, $P < 0.001$). Data are presented as mean ± SEM. $^{***}P < 0.001$. *Scale bar*: 20 μm.

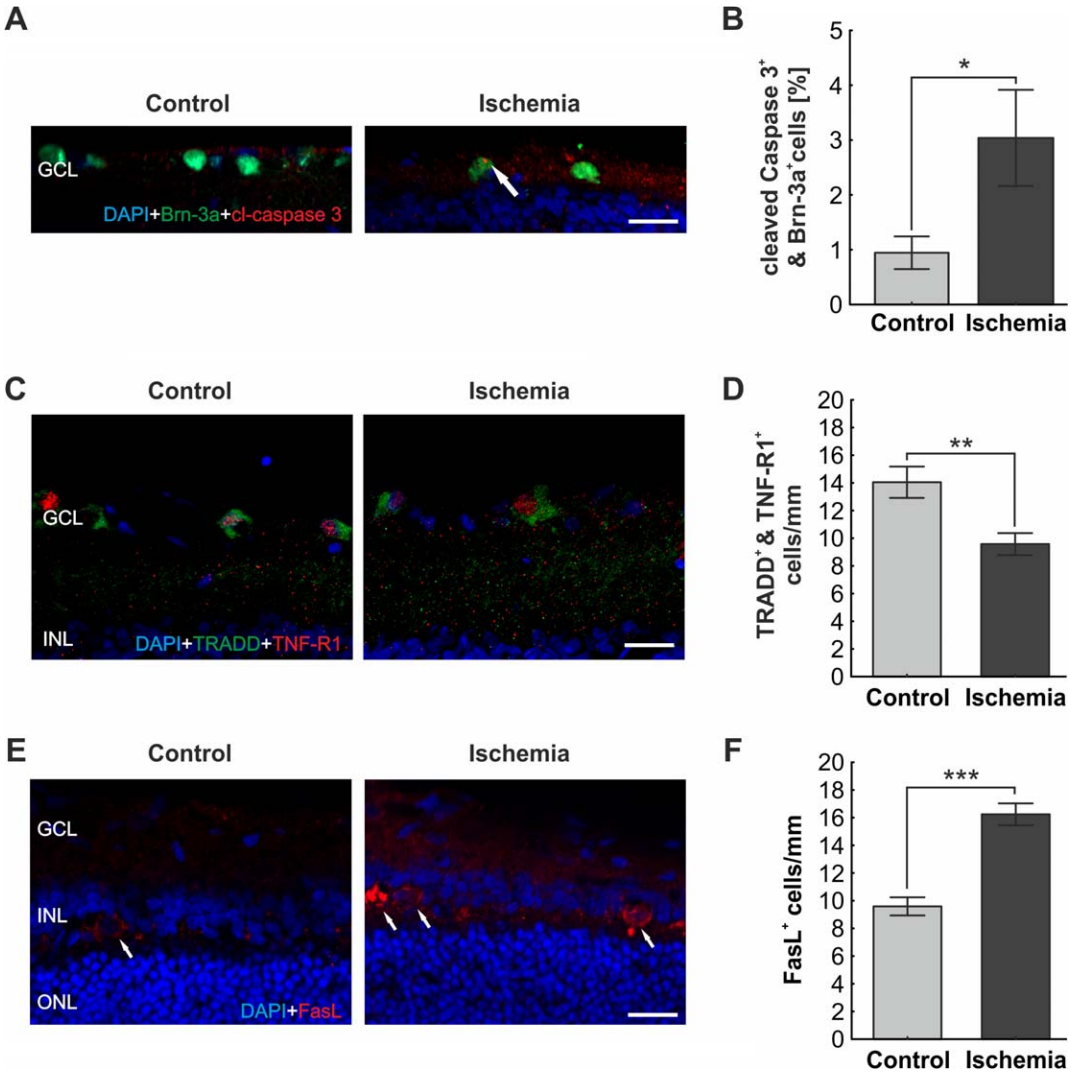

Figure 6. (**A**) Colocalization of Brn-3a (*green*) and cl-caspase 3 (*red*) stained control and ischemic retinas. Only few RGCs were colocalized with activated caspase 3 in ischemic eyes (*arrow*). (**B**) Percentage of cl-caspase 3 colocalized with Brn-3a$^+$ cells (control: 1% ± 0.3%; ischemia: 3% ± 0.9%, $P = 0.0164$). (**C**) Double staining with TRADD (*green*) and TNF-R1 (*red*) in retinas. TRADD and TNF-R1 were present only in the GCL of both groups. (**D**) Fewer colocalization between TRADD and TNF-R1 was visible in ischemic eyes (10 ± 0.8 cells/mm) compared with control eyes (14 ± 1.1 cells/mm, $P = 0.0012$). (**E**) Control and ischemic retinas stained with FasL. FasL$^+$ cells were predominantly detected in the INL of control and ischemic eyes (*arrows*). (**F**) FasL expression was significantly increased in ischemic retinas (control: 10 ± 0.8 cells/mm; ischemia: 16 ± 0.7 cells/mm, $P < 0.001$). Data are presented as mean ± SEM. $^*P < 0.05$. $^{**}P < 0.01$. $^{***}P < 0.001$. *Scale bars*: 20 μm.

in the IPL were stained.[29,30] Cell bodies of cholinergic amacrine cells as well as the stratification in the IPL were mostly lost in ischemic eyes (Fig. 7A). ChAT$^+$ cell counts revealed that cell bodies of cholinergic amacrine cells and the stratification in the inner plexiform layer are mostly lost in ischemic retinas (4 ± 1 cells/mm) compared with control (11 ± 1 cells/mm, $P < 0.001$; Fig. 7B).

No Effect of Ischemia-Reperfusion on Rod Bipolar Cells

Changes in the rod bipolar cells in the ONL were investigated with PKCα. In contrast to the ERG-measurements, where the b-wave was reduced for light intensities ranging from 0.1 to 25 cd/m^2, no obvious difference in the staining pattern of control and ischemic retinas for rod bipolar cells was noted. Dendrites, cell bodies, and axon terminals were equally stained in both groups (Fig. 8A). Quantification of the PKCα$^+$ cell bodies also displayed no difference between both groups (control: 158 ± 5 cells/mm; ischemia: 159 ± 7 cells/mm; $P = 0.9$; Fig. 8B).

Müller Cell and Astrocyte Activity Increased

In order to investigate changes of glia activity of control and ischemic retinas, we examined the expression of GFAP in astrocytes and end feet of Müller cells. Pathological changes, like inflammation or neuronal stress, usually turn glia cells into reactive glia.[31,32] In control retinas, GFAP staining was only observed in the GCL and nerve fiber layer; but in ischemic retinas, the signal reached into the IPL (Fig. 9A). Quantification of the GFAP$^+$ area revealed a significant increase in GFAP expression in ischemic retinas (9.4 ± 1.4) compared with control (3.1 ± 0.3, $P < 0.001$; Fig. 9B). This increased GFAP expression indicates that ischemia is accompanied by an activation of astrocytes. To further investigate changes in the radial glial cells, retinas were stained with vimentin, a marker for an intermediate filament

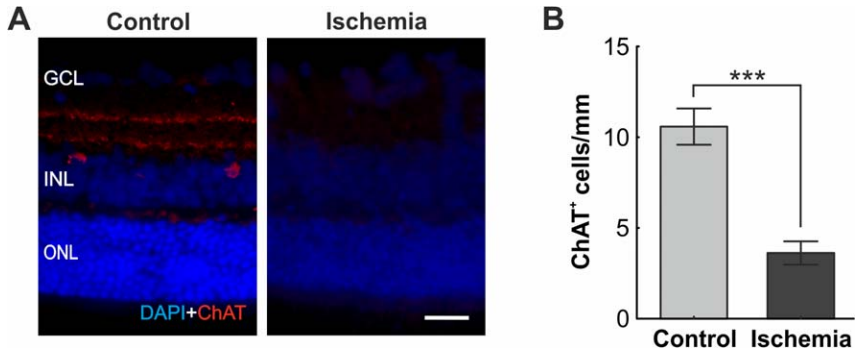

Figure 7. (**A**) ChAT staining in control and ischemic eyes 21 days after ischemia. Cell bodies and stratification (*red*) were present in control, but absent in ischemic eyes. Cell nuclei were stained with DAPI (*blue*). (**B**) The analysis showed a significantly loss of ChAT$^+$ cells in ischemic retinas (control: 11 ± 1 cells/mm; ischemia: 4 ± 1 cells/mm; $P < 0.001$). Data are presented as mean ± SEM. ***$P < 0.001$. *Scale bar*: 20 μm.

present in Müller cells.[33] In both groups, vimentin was present in the end feet and radial structures of Müller cells (Fig. 9C). No significant difference between the groups was noted in regard to the vimentin$^+$ area (control: 9.0 ± 0.6; ischemia: 7.8 ± 0.6; $P = 0.2$; Fig. 9D). The double staining with GFAP and vimentin revealed a distinct staining of the astrocytes with GFAP and Müller cells with vimentin in control retinas (Fig. 9E). After I/R, a colocalization of GFAP and vimentin in the radiary filaments of Müller cells and astrocyte processes is visible (Fig. 9E).

Discussion

In this study, we electrophysiologically and immunohistologically investigated the global effect of transient retinal ischemia on various retinal cell types at 21 days. Besides the RGC and cholinergic amacrine cell loss and a b-wave reduction in the ERG, we also noted a loss of photoreceptor function in the outer retinal layers of ischemic eyes. However, rod bipolar cells appeared to be morphologically intact. Increase of apoptosis and glia activation in the inner retinal layers was also observed, indicating progressing retinal remodeling. We think that after initial I/R damage, a second wave of apoptosis might occur at a later point in time.

Functional Changes

The common method to noninvasively and objectively measure functional changes in the retina is ERG. The a-wave originates by the responses the photoreceptors and the b-wave reflects the responses of amacrine and bipolar cells as well as Müller glia.[17] It has been suggested to use the b-wave as an indicator of severity of ischemic injuries.[34]

In our study, we noted a significant reduction of the a-wave amplitude in ischemic eyes for light intensities ranging from 0.1 to 10 cd/m^2, indicating a disruption of photoreceptor functionality 21 days after I/R ($P < 0.05$; Figs. 2B, 2D). There are diverse reports with regard to a-wave alterations after I/R. For example, while a study using mice reported a reduction of the a-wave amplitude starting at 21 days after I/R, others did not observe this reduction in rats during a 3-month study.[14,35] One of the differences in those two contradicting studies was the experimental method applied to induce ischemia-reperfusion. While one study—were a ligature around the ophthalmic vessels was used to induce ischemia—noted no reduction of the a-wave, elevating the IOP with saline by placing a cannula in the anterior chamber, like in our study, resulted in a reduction of a-wave amplitude.[14,35] Another difference was the use of pigmented or unpigmented animals. It is known that pigmented and unpigmented animals show differences in the retinal metabolism.[36] While the use of pigmented mice caused—similar to our study—a reduction of the a-wave amplitude at 21 days, no changes in the a-wave amplitude could be seen in the study using unpigmented rats.[14,35] Varying approaches to induce ischemia and the use of different animal species and stains leads to discrepancies in the ERG results.

Regarding the b-wave, we saw a significant amplitude reduction for all flash intensities as described by others ($P <$

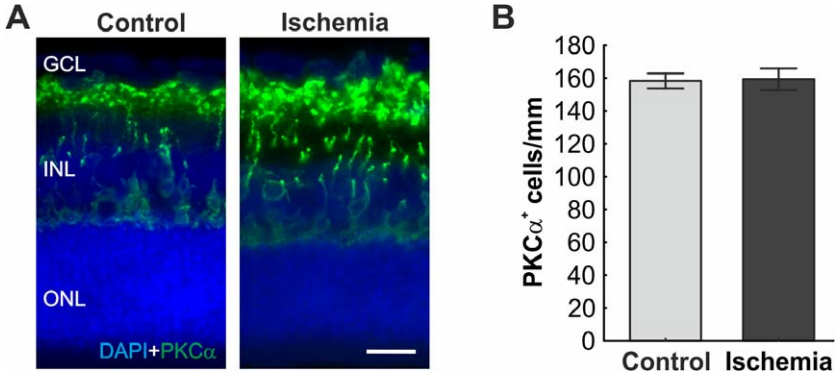

Figure 8. (**A**) Immunohistochemical staining of rod bipolar cells with PKCα in control and ischemic eyes at 21 days, cell bodies, dendrites, and synapses (*green*) are present in both groups. Cell nuclei were stained with DAPI (*blue*). (**B**) Numbers of PKCα$^+$ cells did not differ between the two groups (control: 158 ± 5 cells/mm; ischemia: 159 ± 7 cells/mm; $P = 0.9$). *Scale bar*: 20 μm.

Investigative Ophthalmology & Visual Science

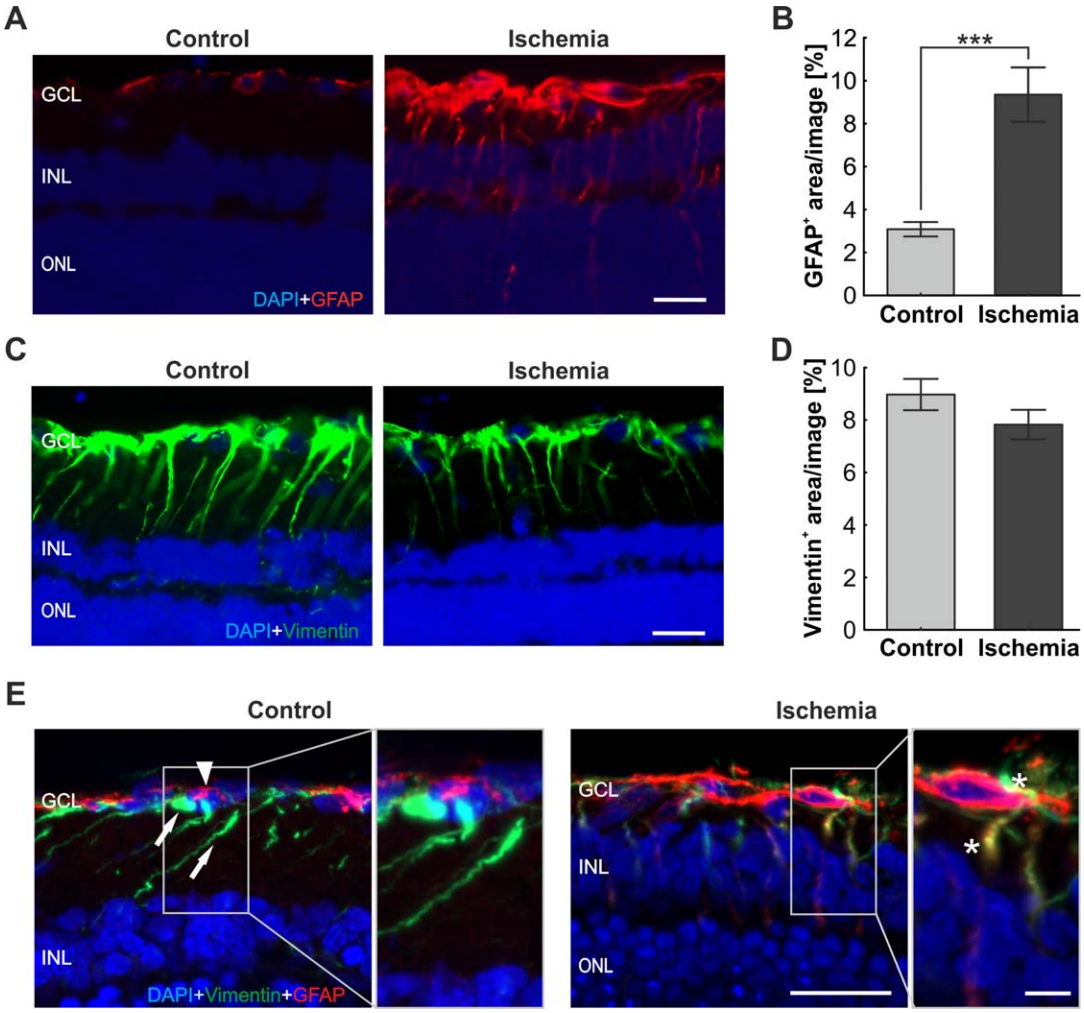

Figure 9. (**A**) Macroglia (GFAP) staining in control and ischemic eyes 21 days after ischemia. In control retinas, GFAP (*red*) was only present in the GCL and nerve fiber layer, while the signal stretched into the IPL of ischemic retinas. Cell nuclei were stained with DAPI (*blue*). (**B**) Ischemic eyes expressed significantly more GFAP protein than control (control: 3.1% ± 0.3%; ischemia: 9.4% ± 1.3%; $P < 0.001$). (**C**) Vimentin staining in control and ischemic eyes. In control and ischemic retinas, vimentin staining (*green*) was present in the end feet in the GCL and radiary filaments up to the INL of Müller cells. Cell nuclei were stained with DAPI (*blue*). (**D**) No significant difference in vimentin$^+$ area could be observed (control: 9.0% ± 0.6%, ischemia: 7.8% ± 0.6%, $P = 0.2$). (**E**) Double staining of GFAP (*green*) and vimentin (*red*). The vimentin stained Müller cells (*arrows*) and GFAP-labeled astrocytes showed no overlap in control retinas. In ischemic retinas, GFAP became colocalized with vimentin in the GCL and radiary filaments of Müller glia, which is shown in detail in the excerpt (*asterisk*). Data are presented as mean ± SEM. ***$P < 0.001$. *Scale bars*: 20 μm (**A**, **C**, **E**), 5 μm (excerpt).

0.001; Fig. 2).[37] Not much is known about latency times of a- and b-wave after ischemia reperfusion. The a-wave latency of ischemic eyes remained unaffected in our study, as previously reported by others.[35] While the b-wave latency in our study did not change, except for the lowest flash intensity, Kim et al. observed some erratic changes in b-wave latency 21 days after I/R.[35] We assume that changes in latency time of b-waves occur at light intensities below 0.1 cd/m^2.

Cellular Changes in the Inner and Outer Retina

The immunohistological and histological results of our study suggest a retinal remodeling is taking place after I/R, especially in the IPL. A significant reduction of the b-wave amplitude was observed in ischemic eyes at all flash intensities, indicating changes in the INL and IPL ($P < 0.001$; Fig. 2C). Although the b-wave mainly represents the responses of rod bipolar cells, it is striking that in contrast to Sun et al., who reported a 16% decrease of rod bipolar cells 2 weeks after I/R, no changes in the cell number and morphology of rod bipolar cells were observed in our study (Figs. 8A, 8B).[38] However, other ischemia-reperfusion studies also noted no alterations of rod bipolar cells after I/R.[39,40] Recently, it has been reported that amacrine cells contribute to the b-wave amplitude.[17] We observed a loss of ChAT$^+$ amacrine cells and its dendrites in the IPL ($P < 0.001$; Fig. 7), which is in accordance with previous studies.[41] This decrease could be either due to a loss of cholinergic amacrine cells and its dendrites or just due to a down-regulation of ChAT.[41,42]

In contrast to amacrine cells and RGCs, rod bipolar cells did not show signs of degeneration. We think the neuronal cells of the inner retina are most affected after an ischemic insult. Additionally, the disruption of cholinergic amacrine cells might affect the b-wave amplitude in a greater way than assumed.

Unlike other reports, no reduction of ONL thickness could be observed in our study.[19,34,38,39] However, the ERG revealed a reduction of the a-wave amplitude in the ischemic group ($P < 0.05$; Fig. 2). This indicates a loss of photoreceptor function after ischemia, which might be an initial sign of damage of the

photoreceptors. This is in accordance with studies that noticed alterations of the outer segments of photoreceptors.[43,44] The changes in the ONL might be due to the use of an albino rat, which are known to have a different retinal metabolism than pigmented animals.[36] Taking our ERG data into account, we assume that photoreceptors are damaged through I/R, but it has not yet affected the synaptic contacts of rod bipolar cells. This might explain why no reduction of the INL could be observed in our study. Morphological changes in rod bipolar cells and a reduction of INL layer thickness can be seen at later points in time.[14,45] However, the differences between retinal ischemic animal models have also to be taken into consideration when investigating changes in retinal morphology.

Apoptosis in the Retina at an Advanced State After Ischemia

Ischemic events led to a stress response and results in a loss of RGC.[10,12] In our study, I/R induced a significant RGC loss ($P = 0.0332$; Fig. 4) and an increase of cl-caspase 3^+ RGCs in ischemic eyes ($P = 0.0164$, Figs. 6A, 6B), indicating that apoptosis plays a major role in the RGC degeneration. This finding was supported by the increase of phagocytes in the GCL ($P < 0.001$; Figs. 5A, 5B), which are known to become activated by neuronal damage or apoptosis.[28] Various reports show a peak of apoptosis 6 to 18 hours after I/R that returns to control level after 48 hours.[10,11,46–48] In our study, we detected an increase of cl-caspase 3 and FasL (Figs. 6E, 6F; $P < 0.001$), as well as a decrease in the colocalization of TNF-R1 and TRADD (Fig. 6D) indicating the presence of apoptotic processes in ischemic retinas at 21 days. Although not much is known about secondary degeneration processes after ischemia, the occurrence of a second wave of neurodegeneration has been shown in cerebral ischemia starting 2 weeks after the initial ischemic insult.[49,50] It is possible that after a primary wave of degeneration 6 to 48 hours after I/R in the INL affecting amacrine cells and RGC, a secondary wave of degeneration starts to take place after I/R at a later point in time affecting other neuronal cells in the INL.[10,11,46,47] A secondary degeneration in the retina has been noted in an optic nerve transection animal model.[51] Partially cutting the optic nerve resulted in a first wave of apoptosis in the projecting area of the cut axons, but also lead to secondary neuronal degeneration in the areas not affected by the initial axon cut starting at 14 days.[51] However, the exact mechanisms of possible secondary degeneration in the retina are not yet understood and are just beginning to be revealed.[52] Further experiments at earlier points in time need to be performed to investigate the appearance of a possible secondary wave of degeneration after I/R similar to cerebral ischemia.

Gliosis in Ischemic Eyes

Under pathological conditions, macroglial cells—like Müller glia and astrocytes—become activated in the retina.[31,32,53] A recent report showed that transient retinal ischemia induced Müller cell gliosis.[35,54] To investigate changes in macroglial cell activity, we examined the expression of GFAP and vimentin on retinal sections 21 days after I/R. In accordance to other reports, we noted an increase of GFAP in ischemic eyes ($P < 0.001$, Figs. 9A, 9B).[35,54,55] The results from our study provide additional support for Müller cell–dependent gliosis after I/R injury.

Conclusions

Investigating different retinal cell types functionally and quantitatively allowed us to directly compare the effects of ischemia on different cells. The whole retina was functionally affected by I/R, while some cells, like bipolar cells, still appeared morphologically intact. It is known that high apoptosis rates are observed immediately after retinal ischemia, which normalizes after 2 days. Yet, we could illustrate that apoptosis is increased in ischemic retinas at 21 days, accompanied by gliosis. The ischemic retina might be affected by secondary apoptotic events.

Acknowledgments

We thank Gesa Stute for technical assistance.

Supported in part by Novartis Pharma GmbH.

Disclosure: **H. Schmid**, None; **M. Renner**, None; **H.B. Dick**, None; **S.C. Joachim**, None

References

1. Osborne NN, Casson RJ, Wood JP, Chidlow G, Graham M, Melena J. Retinal ischemia: mechanisms of damage and potential therapeutic strategies. *Prog Retin Eye Res*. 2004; 23:91–147.
2. Hayreh SS, Zimmerman MB, Kimura A, Sanon A. Central retinal artery occlusion. Retinal survival time. *Exp Eye Res*. 2004;78: 723–736.
3. Hayreh SS. Retinal vein occlusion. *Indian J Ophthalmol*. 1994; 42:109–132.
4. Chen CS, Miller NR. Ocular ischemic syndrome: review of clinical presentations, etiology, investigation, and management. *Compr Ophthalmol Update*. 2007;8:17–28.
5. Wong TY, Mitchell P. Hypertensive retinopathy. *N Engl J Med*. 2004;351:2310–2317.
6. Agarwal R, Gupta SK, Agarwal P, Saxena R, Agrawal SS. Current concepts in the pathophysiology of glaucoma. *Indian J Ophthalmol*. 2009;57:257–266.
7. Osborne NN, Melena J, Chidlow G, Wood JP. A hypothesis to explain ganglion cell death caused by vascular insults at the optic nerve head: possible implication for the treatment of glaucoma. *Br J Ophthalmol*. 2001;85:1252–1259.
8. Bonne C, Muller A, Villain M. Free radicals in retinal ischemia. *Gen Pharmacol*. 1998;30:275–280.
9. Yang Y, Duan JZ, Gui DM, Yang HW, Gao DW. Effect of aminoguanidine on caspase-3 expression in rat retina after ischemia-reperfusion injury. *Int J Ophthalmol*. 2011;4:259–261.
10. Lam TT, Abler AS, Tso MO. Apoptosis and caspases after ischemia-reperfusion injury in rat retina. *Invest Ophthalmol Vis Sci*. 1999;40:967–975.
11. Kurokawa T, Katai N, Shibuki H, et al. BDNF diminishes caspase-2 but not c-Jun immunoreactivity of neurons in retinal ganglion cell layer after transient ischemia. *Invest Ophthalmol Vis Sci*. 1999;40:3006–3011.
12. Mittag TW, Danias J, Pohorenec G, et al. Retinal damage after 3 to 4 months of elevated intraocular pressure in a rat glaucoma model. *Invest Ophthalmol Vis Sci*. 2000;41:3451–3459.
13. Panda S, Jonas JB. [Inner nuclear layer of the retina in eyes with secondary angle-block glaucoma]. *Ophthalmologe*. 1992; 89:468–471.
14. Mayor-Torroglosa S, De la Villa P, Rodriguez ME, et al. Ischemia results 3 months later in altered ERG, degeneration of inner layers, and deafferented tectum: neuroprotection with brimonidine. *Invest Ophthalmol Vis Sci*. 2005;46:3825–3835.
15. Stevens WD, Fortin T, Pappas BA. Retinal and optic nerve degeneration after chronic carotid ligation: time course and role of light exposure. *Stroke*. 2002;33:1107–1112.

16. Ogishima H, Nakamura S, Nakanishi T, et al. Ligation of the pterygopalatine and external carotid arteries induces ischemic damage in the murine retina. *Invest Ophthalmol Vis Sci*. 2011; 52:9710–9720.
17. Weymouth AE, Vingrys AJ. Rodent electroretinography: methods for extraction and interpretation of rod and cone responses. *Prog Retin Eye Res*. 2008;27:1–44.
18. Park SW, Lee HS, Sung MS, Kim SJ. The effect of melatonin on retinal ganglion cell survival in ischemic retina. *Chonnam Med J*. 2012;48:116–122.
19. Joachim SC, Gramlich OW, Laspas P, et al. Retinal ganglion cell loss is accompanied by antibody depositions and increased levels of microglia after immunization with retinal antigens. *PloS One*. 2012;7:e40616.
20. Laspas P, Gramlich OW, Muller HD, et al. Autoreactive antibodies and loss of retinal ganglion cells in rats induced by immunization with ocular antigens. *Invest Ophthalmol Vis Sci*. 2011;52:8835–8848.
21. Blanch RJ, Ahmed Z, Sik A, et al. Neuroretinal cell death in a murine model of closed globe injury: pathological and functional characterization. *Invest Ophthalmol Vis Sci*. 2012; 53:7220–7226.
22. Vickers JC, Costa M. The neurofilament triplet is present in distinct subpopulations of neurons in the central nervous system of the guinea-pig. *Neuroscience*. 1992;49:73–100.
23. Fairless R, Williams SK, Hoffmann DB, et al. Preclinical retinal neurodegeneration in a model of multiple sclerosis. *J Neurosci*. 2012;32:5585–5597.
24. Nadal-Nicolas FM, Jimenez-Lopez M, Sobrado-Calvo P, et al. Brn3a as a marker of retinal ganglion cells: qualitative and quantitative time course studies in naive and optic nerve-injured retinas. *Invest Ophthalmol Vis Sci*. 2009;50:3860–3868.
25. Horstmann L, Schmid H, Heinen AP, Kurschus FC, Dick HB, Joachim SC. Inflammatory demyelination induces glia alterations and ganglion cell loss in the retina of an experimental autoimmune encephalomyelitis model. *J Neuroinflammation*. 2013;10:120.
26. Schmid H, Herrmann T, Kohler K, Stett A. Neuroprotective effect of transretinal electrical stimulation on neurons in the inner nuclear layer of the degenerated retina. *Brain Res Bull*. 2009;79:15–25.
27. Vidal L, Diaz F, Villena A, Moreno M, Campos JG, Perez de Vargas I. Reaction of Muller cells in an experimental rat model of increased intraocular pressure following timolol, latanoprost and brimonidine. *Brain Res Bull*. 2010;82:18–24.
28. Garcia-Valenzuela E, Sharma SC, Pina AL. Multilayered retinal microglial response to optic nerve transection in rats. *Mol Vis*. 2005;11:225–231.
29. Greferath U, Grunert U, Mohler H, Wassle H. Cholinergic amacrine cells of the rat retina express the delta-subunit of the GABAA-receptor. *Neurosci Lett*. 1993;163:71–73.
30. Voigt T. Cholinergic amacrine cells in the rat retina. *J Comp Neurol*. 1986;248:19–35.
31. Kurihara T, Ozawa Y, Shinoda K, et al. Neuroprotective effects of angiotensin II type 1 receptor (AT1R) blocker, telmisartan, via modulating AT1R and AT2R signaling in retinal inflammation. *Invest Ophthalmol Vis Sci*. 2006;47:5545–5552.
32. Peterson WM, Wang Q, Tzekova R, Wiegand SJ. Ciliary neurotrophic factor and stress stimuli activate the Jak-STAT pathway in retinal neurons and glia. *J Neurosci*. 2000;20: 4081–4090.
33. Luna G, Lewis GP, Banna CD, Skalli O, Fisher SK. Expression profiles of nestin and synemin in reactive astrocytes and Muller cells following retinal injury: a comparison with glial fibrillar acidic protein and vimentin. *Mol Vis*. 2010;16:2511–2523.
34. Block F, Schwarz M. The b-wave of the electroretinogram as an index of retinal ischemia. *Gen Pharmacol*. 1998;30:281–287.
35. Kim BJ, Braun TA, Wordinger RJ, Clark AF. Progressive morphological changes and impaired retinal function associated with temporal regulation of gene expression after retinal ischemia/reperfusion injury in mice. *Mol Neurodegener*. 2013; 8:21.
36. Charng J, Nguyen CT, Bui BV, Vingrys AJ. Age-related retinal function changes in albino and pigmented rats. *Invest Ophthalmol Vis Sci*. 2011;52:8891–8899.
37. Jehle T, Wingert K, Dimitriu C, et al. Quantification of ischemic damage in the rat retina: a comparative study using evoked potentials, electroretinography, and histology. *Invest Ophthalmol Vis Sci*. 2008;49:1056–1064.
38. Sun D, Bui BV, Vingrys AJ, Kalloniatis M. Alterations in photoreceptor-bipolar cell signaling following ischemia/reperfusion in the rat retina. *J Comp Neurol*. 2007;505:131–146.
39. Barnett NL, Osborne NN. Prolonged bilateral carotid artery occlusion induces electrophysiological and immunohistochemical changes to the rat retina without causing histological damage. *Exp Eye Res*. 1995;61:83–90.
40. Osborne NN, Larsen A, Barnett NL. Influence of excitatory amino acids and ischemia on rat retinal choline acetyltransferase-containing cells. *Invest Ophthalmol Vis Sci*. 1995;36: 1692–1700.
41. Dijk F, Kamphuis W. An immunocytochemical study on specific amacrine cell subpopulations in the rat retina after ischemia. *Brain Res*. 2004;1026:205–217.
42. Dijk F, Kraal-Muller E, Kamphuis W. Ischemia-induced changes of AMPA-type glutamate receptor subunit expression pattern in the rat retina: a real-time quantitative PCR study. *Invest Ophthalmol Vis Sci*. 2004;45:330–341.
43. Zhang Z, Qin X, Tong N, et al. Valproic acid-mediated neuroprotection in retinal ischemia injury via histone deacetylase inhibition and transcriptional activation. *Exp Eye Res*. 2012;94:98–108.
44. Ju WK, Kim KY, Park SJ, et al. Nitric oxide is involved in sustained and delayed cell death of rat retina following transient ischemia. *Brain Res*. 2000;881:231–236.
45. Cuenca N, Pinilla I, Fernandez-Sanchez L, et al. Changes in the inner and outer retinal layers after acute increase of the intraocular pressure in adult albino Swiss mice. *Exp Eye Res*. 2010;91:273–285.
46. Zhao Y, Niu YJ, Zhou ZY, Gao YX, Wang HY. Expression of Fas/FasL and the apoptosis in rat ischemia/reperfusion - induced retinal injury and effects of bFGF. *Int J Ophthalmol*. 2008;1: 226–229.
47. Zhang W, Liu NN, Xu JH, Liu ZL. HIF-1α expression and retinal cell apoptosis in rat retina ischemia-reperfusion injury. *Int J Ophthalmol*. 2009;2:227–230.
48. Zheng GY, Zhang C, Li ZG. Early activation of caspase-1 after retinal ischemia and reperfusion injury in mice. *Chin Med J (Engl)*. 2004;117:717–721.
49. Wang F, Xing S, He M, et al. Nogo-A is associated with secondary degeneration of substantia nigra in hypertensive rats with focal cortical infarction. *Brain Res*. 2012;1469:153–163.
50. Lin B. Encephalopathy: a vicious cascade following forebrain ischemia and hypoxia. Cent *Nerv Syst Agents Med Chem*. 2013;13:57–70.
51. Levkovitch-Verbin H, Dardik R, Vander S, Melamed S. Mechanism of retinal ganglion cells death in secondary

Investigative Ophthalmology & Visual Science

degeneration of the optic nerve. *Exp Eye Re*s. 2010;91:127–134.

52. Krizaj D, Ryskamp DA, Tian N, et al. From mechanosensitivity to inflammatory responses: new players in the pathology of glaucoma. *Curr Eye Res*. 2014;39:105–119.
53. Bargagna-Mohan P, Paranthan RR, Hamza A, et al. Withaferin A targets intermediate filaments glial fibrillary acidic protein and vimentin in a model of retinal gliosis. *J Biol Chem*. 2010;285:7657–7669.
54. Hirrlinger PG, Ulbricht E, Iandiev I, Reichenbach A, Pannicke T. Alterations in protein expression and membrane properties during Muller cell gliosis in a murine model of transient retinal ischemia. *Neurosci Lett*. 2010;472:73–78.
55. Wurm A, Iandiev I, Uhlmann S, et al. Effects of ischemia-reperfusion on physiological properties of Muller glial cells in the porcine retina. *Invest Ophthalmol Vis Sci*. 2011;52:3360–3367.

Investigative Ophthalmology & Visual Science